A Novel Frequency Synchronization Algorithm and its Cramer Rao Bound in Practical UWB Environment for MB-OFDM Systems

Debarati SEN [1], *Rahul DASGUPTA*[2], *Saswat CHAKRABARTI* [1], *R. V. RAJA KUMAR*[2]

[1] G. S. S. School of Telecommunications, Indian Institute of Technology Kharagpur, Pin-721302, India
[2] Dept. of E&ECE, Indian Institute of Technology Kharagpur, Pin-721302, India

debarati@gssst.iitkgp.ernet.in

Abstract. *This paper presents an efficient time-domain coarse frequency offset (FO) synchronizer (TCFS) for multi-band orthogonal frequency division multiplexing (MB-OFDM) systems effective for practical ultra-wide-band (UWB) environment. The proposed algorithm derives its estimates based on phase differences in the received subcarrier signals of several successive OFDM symbols in the preamble. We consider different carrier FOs and different channel responses in different bands to keep the analysis and simulation compatible for practical multi-band UWB scenario. Performance of the algorithm is studied by means of bit error rate (BER) analysis of MB-OFDM system. We derive the Cramer Rao lower bound (CRLB) of the estimation error variance and compare it with the simulated error variance both in additive white Gaussian noise and UWB channel model (CM) environments, CM1-CM4. Both analysis and simulation show that TCFS can estimate coarse carrier FO more efficiently in UWB fading channels for MB-OFDM applications compared to the other reported results in literature. Also, computational complexity of the proposed algorithm is analyzed for its usability evaluation.*

Keywords

Synchronization, MB-OFDM, Ultra-Wideband, Frequency offset correction, Cramer Rao Bound.

1. Introduction

Multi-band orthogonal frequency division multiplexing (MB-OFDM) based transmission for ultra-wideband (UWB) [1] is commercially successful for high speed wireless personal area networks (WPAN). It offers enhanced coexistence with traditional and protected radio services by dynamical turn on/off of subcarriers.

While MB-OFDM is enriched with all the merits of OFDM, it suffers (also due to OFDM) from inherent sensitivity to frequency synchronization errors which causes a loss of orthogonality among subcarriers and leads to severe degradation in error performance [2]. In an MB-OFDM system, frequency synchronization becomes even more critical due to the combination of high data rate and fast frequency hopping (FH) of OFDM symbols over bands which finally demands a low complexity, fast converging algorithm in practice.

Synchronization for OFDM systems over fading channels is well investigated over last two decades and several synchronization algorithms have been proposed in the literatures [2]-[8]. The frequency offset (FO) estimation algorithms for MB-OFDM system is reported in [9]-[16]. Kato et al. [9] reports a frequency offset compensation scheme by symbol mapping at frequency spreading which confirms the reduction of ICI on the pilot subcarriers. But, neither any mathematical analysis in support of the scheme nor any simulation in a realistic UWB environment is provided in [9]. Yak et al. [10] derived the maximum likelihood (ML) estimator for FO following [2] using the last two successive OFDM symbols of the packet synchronization (PS) sequence of the preamble after timing synchronization. The Cramer Rao Lower Bound (CRLB) for ML FO estimator was also calculated and compared with simulated results for the UWB channel models (CM) CM1 and CM2. However, the performance of the MB-OFDM system with FO correction is not analyzed. Li et al. [11] proposed the Best Linear Unbiased Estimator (BLUE) for oscillator FO estimation for MB-OFDM based UWB. Following the same method of [11], Jacobs et al. [12] presented the BLUE estimator for a variable correlation window. Li et al. has extended the BLUE estimator for time-variant channels in [13]. But, in an indoor WPAN environment, the Doppler shift that exists is very small and hence its effect can be neglected[1]. Png et al. [14] presented a joint carrier and sampling FO estimation scheme considering a common error source for both. But, performance analysis of the proposed estimator in terms of error variance is not derived in this paper [14].

[1] In an indoor WPAN, the frequency spreading due to Doppler is mainly contributed by pedestrian speed. This spreading may be in the order of 10 Hz. For this spreading to matter, the time elapsed needs to be of the order of several tens of mille second. In view of this long time, the frequency offset due to Doppler spreading can be avoided.

We reported the performance of the MB-OFDM system with a new FO correction method for CM1-CM4 in [15] and [16]. In [15], we considered the same amount of normalized carrier FO in all three bands of band group 1 (BG 1) of the MB-OFDM system. We also provided the CRLB on the estimation error in an AWGN channel. In [16], we considered different carrier FOs over different bands which is a much more practical approach in a real UWB environment compared to the consideration in [15] and modified our analysis. However, behavior of the estimation error variance and its CRLB in UWB channels are not verified in [15] and [16].

In this paper, we describe our algorithm from [15] considering the realistic approach of [16] and we derive the CRLB on estimation error variance in all CMs (CM1-CM4) which are supported by simulation. The proposed algorithm closely follows the scheme of Schmidl et al. [4] and considers different normalized carrier FOs and different channel frequency responses in three different bands. Throughout the paper, we refer to this proposed estimator ([15], [16]) as time domain coarse frequency offset synchronizer (TCFS). The CRLB on the variance of FO estimation error is derived from the Fisher information matrix (FIM) to show the efficiency of our scheme. We compare the CRLB and error variance from simulation studies with that reported by Yak et al[2]. [10] to show its superiority over that given in [10]. Bit Error Rate (BER) performances, as obtained by simulation studies over CM1-CM4 are presented. We also incorporate the analysis of the algorithmic computational complexity for TCFS. Our major findings here are summarized as follows:

In AWGN Channel :

- The variance of estimation errors of the proposed estimator (TCFS) decreases with the increase of number (no.) of OFDM symbols L (received in a particular band in a band group) utilized in estimation.
- Error variance as obtained from simulation for TCFS matches closely to that of theoretical CRLB for different OFDM symbols viz. L =2, 3, 4, and 6.

In UWB Channel :

- CRLB in UWB environment is scaled version of CRLB in AWGN channel. The scaling factor is having its value <1. Its value is near to 1 for UWB CM1 which is line-of-sight (LOS) channel and minimum for CM4 which is non-line-of-sight (NLOS) channel. As a result, CRLB plot for CM1 is near to AWGN case study followed by CM2-CM4.
- The BER performance of MB-OFDM system with TCFS estimator shows that with higher number of iterations of estimation algorithm i.e. using greater no. of OFDM symbols, say L = 6, the performance reaches closely to that of AWGN performance. Compared to L = 2 and L = 3, TCFS with L = 6 improves the Eb/No (Eb = bit energy, No/2 = noise power spectral density) of around 8.0 dB and 4.0 dB respectively in CM1-CM4 at the BER of 2×10^{-4}. This performance is achieved with a calculated computational complexity of $\{(2W+N)(L\text{-}1)\text{-}1\}/T_{\text{total}}$ additions /sec and $(L\text{-}1)N/T_{\text{total}}$ multiplications/sec; where N is the size of FFT, W is no. of stages of the CORDIC block (used for extraction of phase), T_{total} = total run time for estimation.

Comparative study with existing reported result:

- We compare the derived CRLB for both TCFS with that of reported results in [10] for both CM1 and CM2. For both the CMs we find that the calculated as well as simulated results for error variance perform better than depicted in [10] in the low signal-to-noise ratio (SNR) zone (SNR ≤ 8 dB). For example, at the error variance of 10^{-4}, we observe SNR improvement of 2.8 dB and 1.3 dB relative to [10] in CM1 and CM2 respectively with TCFS. As the preferable application of UWB is in low SNR region, our synchronizer TCFS seems to be attractive in practice.

The rest of the paper is organized as follows: Section 2 briefly presents the system description, the UWB channel model and the signal model, and sets the background. Our frequency offset estimation scheme TCFS is analyzed in Section 3 and its CRLB both in the AWGN and the UWB channel is derived in Section 4. The Simulation results, the relevant discussions, and the algorithmic computational complexity analysis are given in Section 5. We conclude with the summary of our study in Section 6.

2. Model of the MB-OFDM System

2.1 The MB-OFDM System

MB-OFDM splits the UWB spectrum into several bands[3] of 528MHz each and transmits OFDM symbols by hopping over RF frequency bands following a fixed time frequency interleaved (TFI) pattern. In the MB-OFDM proposal of ECMA-368 [17], a standard preamble is provided to aid receiver algorithms related to coarse and fine time-frequency synchronization and channel estimation. The first 21 identical OFDM symbols, called PS sequences are followed by 3 identical OFDM symbols provided for frame synchronization (FS) followed by 6 channel estima-

[2] To the best of our knowledge, CRLB for UWB channels (CM1 and CM2) are reported in literature by Yak et al. [10] only.

[3] ECMA-368 [17] splits the whole UWB spectrum into fourteen (14) bands. The first twelve (12) bands are then grouped into four (4) band groups with three bands in each. The fifth band group is having remaining two bands. In order to comply with world-wide regulations, a sixth band group consisting of three bands is defined within first four band group (refer: Section 11.1.2 of [17]).

tion (CE) sequences. PS sequences are assigned for packet detection, AGC stabilization, timing synchronization and frequency synchronization. FS and CE are dedicated for synchronization of the receiver algorithm within the preamble and channel estimation along with fine time-frequency estimation respectively. PS and FS sequences have the same magnitude but opposite polarity.

2.2 UWB Channel Model

The IEEE 802.15 channel modeling sub-committee [18] adopted the modified Saleh-Valenzuela (S-V) model for UWB that can uniquely distinguish between "cluster arrival rates" and "ray arrival rates" (Fig. 1). Depending on the distance of transmission, four different kinds of channel models are described in [18]: CM1 is 0-4m LOS channel; CM2 is 0-4m NLOS channel; CM3 is 0-10m NLOS channel; and CM4 is the channel with 25nsec rms delay spread. UWB channels contribute to the frequency dependent dispersive effects [19]-[21] of the transmitted signal. In view of the dispersive nature, the channel characteristics as applicable in different frequency bands differ significantly. The model of the impulse response (IR) of a RF UWB channel is given in [18]. Its equivalent complex base band impulse response component (CIR) applicable for band *'b'* can be written as [11]

$$h_b(i) = \chi \sum_{u=0}^{U} \sum_{v=0}^{V} \alpha_{v,u} e^{-j2\pi f_b (T_u + \tau_{v,u})} p(iT_s - T_u - \tau_{v,u} - t_0) \;;\; 0 \le i \le L_b - 1 \quad (1)$$

where $p(t)$ is the impulse response of the combined transmit-receive filter with a delay of t_0 introduced to satisfy causality; T_s is the sampling time; L_b is the length of CIR; f_b is the carrier frequency in band *'b'*; χ, $\alpha_{v,u}$, $T_u, \tau_{v,u}$ are the log-normal shadowing, the log-normally distributed multipath gain coefficient, the delay of u-th cluster, and the delay of v-th ray related to u-th cluster arrival time respectively.

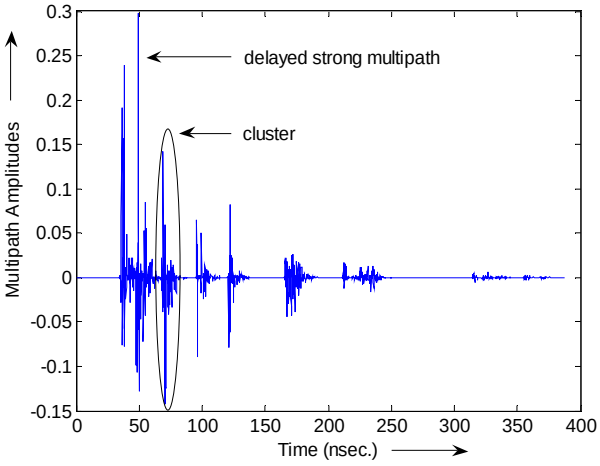

Fig. 1. Impulse Response of UWB Channel with non-overlapping clusters.

2.3 The Signal Model and Effect of the Frequency Offset

Let $\{X(k)\}$ represent the complex serial stream of symbols to be transmitted using OFDM. The complex base band OFDM symbol may be represented as

$$x(t) = \frac{1}{N} \sum_{k=0}^{N-1} X(k) e^{j2\pi kft}, 0 \le t < T \text{ and } 0 \le k < N \quad (2)$$

where f is the inter subcarrier spacing.

The modulated signal is sampled with a sampling interval T/N. To reduce the effect of inter symbol interference (ISI) due to multi-path, the N length IFFT output is padded with N_g zero valued samples such that the total samples in one MB-OFDM symbol is $N_S = N + N_g$. Considering an indoor WPAN, where Doppler shift is negligible, the carrier FO is solely attributed to the mismatch of crystal oscillators at the transmitter and receiver. Assuming a normalized carrier frequency offset (NCFO) of $\varepsilon_b = \Delta f_b / f$, where Δf_b is the frequency offset in band 'b'; a UWB channel transfer function coefficient related to k-th subcarrier corresponding to l-th OFDM symbol for band 'b' given by $H_b(l,k)$; and $X(l,k)$ be the information transmitted over k-th subcarrier of l-th OFDM symbol; the n-th sample of l-th received OFDM symbol in band 'b' can be represented as

$$y_b(l,n) = \frac{1}{N} \sum_{k=0}^{N-1} X(l,k) H_b(l,k) e^{\frac{j2\pi fk\left(n - N_g - lN_s\right)T}{N}} e^{j2\pi\varepsilon_b n/N} + w_b(l,n) \quad (3)$$

where $w_b(l,n)$ is the n-th time domain AWGN sample added to l-th OFDM symbol in band 'b' with mean zero and variance σ^2.

After overlap and add operation, the zero padded portions are removed from an OFDM symbol for further signal processing. Hence, (3) can also be expressed as

$$y_b(l,n) = e^{j2\pi\varepsilon_b (n + N_g + lN_s)/N} x_b(l,n) + w_b(l,n) \quad (4)$$

where

$$x_b(l,n) = \frac{1}{N} \sum_{k=0}^{N-1} X(l,k) H_b(l,k) e^{\frac{j2\pi kn}{N}} \quad (5)$$

$x_b(l,n)$ is the n-th time domain sample of the l-th OFDM symbol. The distance (D_b) between the n-th samples of two successively received OFDM symbols in a band 'b' given as $D_b = dN_S$, depends on the TFI pattern opted for transmission; where, for TFI 1 and 2, d = 3; for TFI 3 and 4, d =1 and 5; for TFI 5 to 7, d=1; for TFI 8 to 10 d =2 (Fig. 2). In (5), it is observed that ε_b causes a phase rotation of $2\pi\varepsilon_b(n+N_g+lN_S)/N$. If it remains uncorrected, it causes both rotation of constellation points and a spread of the constellation points on each subcarrier.

After Fast Fourier Transformation (FFT) of (4), signal in frequency domain is written after simplification as [22]

$$Y_b(l,q) = e^{j2\pi\varepsilon_b(N_g+lN_s)/N} X(l,(q-\varepsilon_b))H_b(l,q) + \sum_{n=0}^{N-1} w_b(l,n)e^{-j2\pi nq/N} \quad (6)$$

It is observable from (6) that the performance fall gradually increases with FO (Δf_b) when $|\Delta f_b| < f/2$ while it results in a complete detection error when $|\Delta f_b| > f/2$. Hence, FO correction is an essential and crucial issue.

FO synchronization may be performed in the receiver in the time domain before performing FFT of incoming signal either by cyclic extension or by using special training symbols. Synchronization techniques based on cyclic extension are not suitable for high rate packet transmission (i.e. MB-OFDM) as, (i) An accurate synchronization needs an averaging over large (>10) nos. of OFDM symbols to attain distinct no. of peaks and a reasonable SNR. (ii) For efficient data transmission, the synchronization time needs to be as short as possible. In the next Section we discuss our proposed training based FO estimation algorithm.

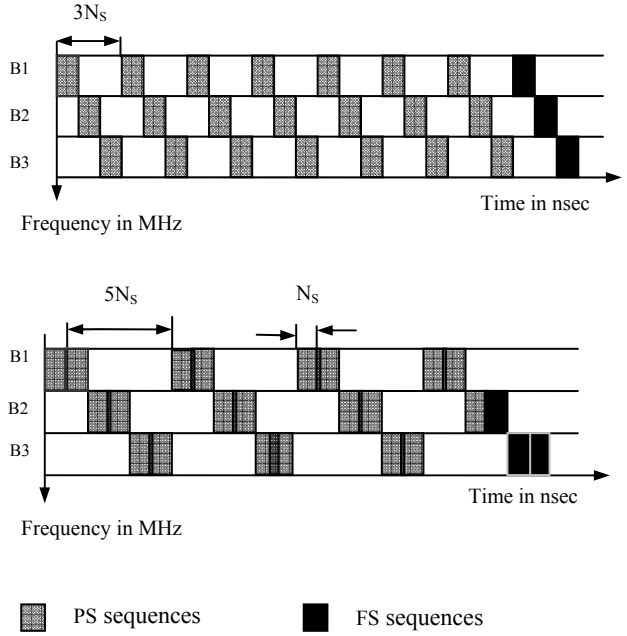

Fig. 2. OFDM symbol hopping pattern over three bands of BG1 for a) TFI 1 and b) TFI 3.

3. The Proposed Frequency Offset Estimation Algorithm (TCFS)

As per MB-OFDM specification [17], the maximum tolerances for transmitter and receiver frequency are ±20 parts per million (ppm) and the inter subcarrier spacing is f = 4.125MHz. The carrier frequencies of band1, band2, and band3 generated from source oscillator are 3432 MHz, 3960 MHz, and 4488 MHz respectively. Hence, the 40 ppm at the three carrier frequencies yields FOs of 137.28 kHz, 158.40 kHz, and 179.52 kHz. So, the maximum NCFO in three bands are ε_1=0.033, ε_2=0.038, and ε_3=0.043 respectively.

In MB-OFDM, the center carrier frequencies of three bands (in BG1) say f_1, f_2, and f_3 are typically generated from the same source oscillator frequency say f_0, so that, $f_1=\alpha_1 f_0$, $f_2=\alpha_2 f_0$, and $f_3=\alpha_3 f_0$, where, α_1, α_2, and α_3 are the scale factors of the corresponding three bands respectively. Thus the frequency offsets in the three bands (in absence of Doppler) are fully related. Therefore, FO estimated in any one band can easily be extended to estimate the offsets in other bands. Our proposed scheme TCFS is based on this illustration.

3.1 TCFS Algorithm

Assuming perfect timing synchronization, TCFS algorithm estimates the FO in time-domain. It utilizes the last 'L' OFDM symbols of the dedicated training symbols for synchronization in the preamble received in one band. We assume that, the FO is initially estimated in the band, say *'b_{in}'*. The estimator accumulates the phase offsets comparing several successive OFDM symbols in *'b_{in}'* in two steps: firstly, along the samples of a pair of OFDM symbols by performing complex conjugate multiplication of two successive OFDM symbols received in that band, and then repeating the computation over several sets of OFDM symbol pairs received in the same band. FO is estimated by averaging[4] the accumulated phase over total no. of OFDM samples considered for offset estimation in a band.

Complex conjugate multiplication of n-th sample of the l-th and (l+d)-th OFDM symbol (which are dN_S samples apart from each other) in band *'b_{in}'* can be expressed as

$$Z_{b_{in}}(l,n) = e^{j2\pi\varepsilon_{b_{in}} dN_S/N} x^*_{b_{in}}(l,n)x_{b_{in}}\left((l+d),n\right) + \bar{w}_{b_{in}}(l,n) \quad (7)$$

where $\varepsilon_{b_{in}} \in \varepsilon_b$, and $b_{in} \in b \in [1,2,....14]$.

Considering $\bar{w}_{b_{in}}(l,n)$ as the effective noise component of the complex conjugate product given by

$$\begin{aligned}\bar{w}_{b_{in}}(l,n) = {} & e^{-j2\pi\varepsilon_{b_{in}}(n+N_g+lN_s)/N} x^*_{b_{in}}(l,n)w_{b_{in}}((l+d),n) \\ & + e^{j2\pi\varepsilon_{b_{in}}(n+N_g+(l+d)N_s)/N} x_{b_{in}}((l+d),n)w^*_{b_{in}}(l,n) \\ & + w^*_{b_{in}}(l,n)w_{b_{in}}((l+d),n)\end{aligned} \quad (8)$$

Using the fact that $X(l,k) = X(l+d,k)$ (as discussed in Section 2.1, the 21 transmitted training OFDM symbols for synchronization are identical), and assuming that the channel is time invariant during one frame (Preamble+ Header+ Payload) transmission i.e. $H_{b_{in}}(l,k)=H_{b_{in}}(l+d,k)$, on further simplification of (7), we get

$$Z_{b_{in}}(l,n) = e^{j2\pi\varepsilon_{b_{in}} N_s d/N} \left|x_{b_{in}}(l,n)\right|^2 + \bar{w}_{b_{in}}(l,n) \; . \quad (9)$$

[4] In order to reduce the effect of noise.

The phase offset $\hat{\phi}_{b_{in}}(l)$ estimated from pair of M samples of the l-th and $(l+d)$-th OFDM symbol in band *'b_{in}'* is represented as

$$\hat{\varphi}_{b_{in}}(l) = \frac{2\pi N_S d\varepsilon_{b_{in}}}{N} + \arg\sum_{n=0}^{M-1} \overline{w}_{b_{in}}(l,n). \quad (10)$$

Estimated FO $\hat{\varepsilon}_{b_{in}}(l)$ from the two consecutively received OFDM symbols l and $(l+d)$ in band *'b_{in}'* can be written as

$$\hat{\varepsilon}_{b_{in}}(l) = \varepsilon_{b_{in}} + \frac{\arg\sum_{n=0}^{M-1} \overline{w}_{b_{in}}(l,n)}{2\pi \frac{N_s}{N} d}. \quad (11)$$

The no. of estimations using L OFDM symbols will be $(L\text{-}1)$. The estimated frequency offset $\hat{\varepsilon}_{b_{in}}(L)$ using last L OFDM symbols of the preamble may be represented as

$$\hat{\varepsilon}_{b_{in}}(L) = \varepsilon_{b_{in}} + \frac{\frac{1}{(L-1)}\left(\sum_{l=1}^{L-1} \arg\sum_{n=0}^{M-1} \overline{w}_{b_{in}}(l,n)\right)}{2\pi \frac{N_s}{N} d}. \quad (12)$$

It can be easily shown that, the frequency offset estimation in any other frequency band ($\hat{\varepsilon}_b$) of the MB-OFDM system can be obtained from the initially estimated offset $\hat{\varepsilon}_{b_{in}}(L)$ as

$$\hat{\varepsilon}_b = (C_b / C_{est})\,\hat{\varepsilon}_{b_{in}}(L) \quad (13)$$

where C_b is the center carrier frequency of the band for which the FO needs to be estimated, and C_{est} is the center carrier frequency of the band at which the initial FO, $\hat{\varepsilon}_{b_{in}}(L)$ is estimated. In the next Section, we calculate the variance of frequency offset estimation.

3.2 Variance of Estimation Error

A detailed derivation of the variance of the frequency offset estimation is given in Appendix A. As shown in (49) in Appendix A, the estimation variance from two consecutive OFDM symbols may be presented as

$$Var\left(\hat{\varepsilon}_{b_{in}}(l)\right) = \frac{N^2}{(2\pi)^2 d^2 N_s^2 M(SNR)}. \quad (14)$$

The variance of the estimated FO from L symbols as expressed in (50) in Appendix A is

$$Var\left(\hat{\varepsilon}_{b_{in}}(L)\right) = \frac{N^2}{(2\pi)^2 (L-1) d^2 N_s^2 M(SNR)}. \quad (15)$$

It is observed from (20) that the variance of the FO estimate decreases with the increase of number of OFDM symbols (L) used for FO estimate, distance between two successively received OFDM symbols in a band, and signal-to-noise-ratio (SNR). In order to verify the efficiency of the proposed estimator, we derive the CRLB of the estimate in Section 4.

3.3 Algorithmic Computational Complexity of TCFS

The detailed calculation of the complexity analysis is shown in Appendix B. We define : $T_{\text{total}}$is the total time period during which estimation runs, L is the no. of symbols utilized for estimation per band, N is the length of FFT window, and W is the no. of stages of the CORDIC block (used for extraction of the phase, Appendix B).

Then, total multiplication and additional complexity for TCFS given by (53) and (54) in Appendix B are as

$$(L-1)N / T_{total} \;\; multiplications/sec$$

$$\{(2W+N)(L-1)-1\} / T_{total} \;\; additions/sec \quad (16)$$

4. Cramer Rao Lower Bound (CRLB) of the Estimation Error

It is a useful and general practice in signal processing feasibility studies to place a lower bound on the variance of any unbiased estimator.

4.1 CRLB for AWGN Channel

To derive the Cramer Rao Bound of the estimated FO, we rewrite (7) as

$$Z_{b_{in}}(l,n) = U_{b_{in}}(l,n) + jV_{b_{in}}(l,n) \quad (17)$$

where

$$U_{b_{in}}(l,n) = A\cos(2\pi\varepsilon_{b_{in}} dN_s / N) + \overline{w}_{in,b_{in}}(l,n),$$

$$V_{b_{in}}(l,n) = A\sin(2\pi\varepsilon_{b_{in}} dN_s / N) + \overline{w}_{qp,b_{in}}(l,n),$$

where in

$$A = \left|x_{b_{in}}(l,n)\right|^2 \quad (18)$$

$\overline{w}_{in,b_{in}}(.)$ and $\overline{w}_{qp,b_{in}}(.)$ are the in-phase and q-phase components of the effective noise of the complex conjugate product ($\overline{w}_{b_{in}}(l,n)$) respectively obtained from (7). Now, we want to estimate the parameter vector

$$\alpha = [A, \varepsilon_{b_{in}}]^T. \quad (19)$$

The joint probability density function of $Z_{b_{in}}(l,n)$ is

$$f(Z_{b_{in}}(l,n),\alpha) = \left(\frac{1}{2\pi\sigma^2}\right)^M e^{-\frac{1}{2\sigma^2}\left[\sum_{n=0}^{M-1}\left(U_{b_{in}}(l,n)-U(n)\right)^2+\left(V_{b_{in}}(l,n)-V(n)\right)^2\right]} \quad (20)$$

where

$$U(n)=A\cos\left[2\pi\varepsilon_{b_{in}}d\frac{N_s}{N}\right]\text{ and }V(n)=A\sin\left[2\pi\varepsilon_{b_{in}}d\frac{N_s}{N}\right] \quad (21)$$

Unbiased CRLB is obtained from diagonal elements of Inverse FIM $J(\alpha)$ [23] which is given as

$$J(\alpha)=\begin{bmatrix}-E\left[\dfrac{\partial^2\ln\left(f\left(Z_{b_{in}}(l,n);\alpha\right)\right)}{\partial A^2}\right] & -E\left[\dfrac{\partial^2\ln\left(f\left(Z_{b_{in}}(l,n);\alpha\right)\right)}{\partial A\partial\varepsilon_{b_{in}}}\right]\\ -E\left[\dfrac{\partial^2\ln\left(f\left(Z_{b_{in}}(l,n);\alpha\right)\right)}{\partial\varepsilon_{b_{in}}\partial A}\right] & -E\left[\dfrac{\partial^2\ln\left(f\left(Z_{b_{in}}(l,n);\alpha\right)\right)}{\partial\varepsilon_{b_{in}}^2}\right]\end{bmatrix} \quad (22)$$

Detail calculations for obtaining the different elements of matrix (22) are shown in Appendix C. Also, CRLB for variance of estimation error for two consecutive OFDM symbols are given in (65) in Appendix C.

When FO is estimated over L OFDM symbols, the CRLB for variance of FO estimation error is

$$Var\left(\hat{\varepsilon}_{b_{in}}(L)\right)=N^2/\{(SNR)M(L-1)\left(2\pi dN_s\right)^2\}. \quad (23)$$

4.2 CRLB for UWB Channel

It is described in Section 2.2 that the gain co-efficient of UWB channel $\alpha_{i,j}$ is log-normally distributed such that

$$20\log(|\alpha_{i,j}|)\sim Normal(\mu_{i,j},\sigma_1^2+\sigma_2^2) \quad (24)$$

$$\text{where }\mu_{i,j}=\frac{10\ln\Omega_0-10T_j/\Gamma-10\tau_{i,j}/\gamma}{\ln 10}-\frac{\sigma_1^2+\sigma_2^2}{20}. \quad (25)$$

Here, Γ and γ are the cluster and the ray decay rates respectively and Ω_0 is the mean energy of the first path of the first cluster. Also, $\sigma_1=\sigma_2=3.3941$ dB. The cluster arrival time T_j and the ray arrival time $\tau_{i,j}$ follows Poisson distribution. Their probability distribution function are given by

$$p\left(T_j|T_{j-1}\right)=\Lambda\exp\left[-\Lambda\left(T_j-T_{j-1}\right)\right],\quad j>0, \quad (26)$$

$$p\left(\tau_{i,j}|\tau_{(i-1),j}\right)=\lambda\exp\left[-\lambda\left(\tau_{i,j}-\tau_{(i-1),j}\right)\right],\quad i>0 \quad (27)$$

where Λ is the cluster arrival rate, λ is Ray arrival rate, i.e. the arrival rate of path within each cluster and, $\lambda >> \Lambda$. Now, suppose there is a total of P no. of rays in the channel IR. Thus, each sample of an OFDM symbol, X_n would pass through P multipath. Thus, the received sample

$$X_{nR}=X_n\sum_{p=0}^{P-1}\alpha_p \quad (28)$$

Here, $|\alpha_p|$ the impulse magnitude of the i-th ray of the j-th cluster represents the amplitude attenuation of the OFDM sample in the p-th multipath. So, $|\alpha_p|$ can also be represented as

$$|\alpha_p|=\exp(\xi y_p) \quad (29)$$

where $y_p \sim Normal(\mu_p,\sigma^2_p)$ and $\xi=\ln(10)/20$.

Again, from (24) and (25)

$$\mu_p=\mu_{i,j}\quad\text{and}\quad\sigma_p^2=\sigma_1^2+\sigma_2^2. \quad (30)$$

Now, the total amplitude attenuation β, of the received sample X_{nR}, is given by

$$\beta=\sum_{p=0}^{P-1}\alpha_p=\sum_{p=0}^{P-1}\exp(\xi y_p). \quad (31)$$

Now, since α_p is log normally distributed, β is a sum of independent log-normal variables. Such a sum can be approximated by another log normal random variable by Wilkinson's Method of approximation [24], [25] given as

$$\beta=\exp(z)\qquad\text{where}\quad z\sim Normal(\mu_z,\sigma_z^2). \quad (32)$$

The mean and variance of the random variable β, μ_β and σ^2_β can be obtained as [26]

$$\mu_\beta=E[\beta]=E[\sum_{p=0}^{P-1}\exp(\xi y_p)], \quad (33)$$

$$\begin{aligned}\sigma_\beta^2&=E[\beta^2]-\left(E[\beta]\right)^2\\&=E[\sum_{p=0}^{P-1}\exp(2\xi y_p)]-\left(E[\sum_{p=0}^{P-1}\exp(\xi y_p)]\right)^2.\end{aligned} \quad (34)$$

Thus, μ_β and σ^2_β can be related to μ_p and σ^2_p [23] as

$$\mu_\beta=\sum_{p=0}^{P-1}\exp\left(\xi\mu_p+\xi^2\frac{\sigma_p^2}{2}\right), \quad (35)$$

$$\begin{aligned}\sigma_\beta^2=&\sum_{p=0}^{P-1}\exp\left(2\xi\mu_p+2\xi^2\sigma_p^2\right)\\&+2\sum_{p=0}^{P-2}\sum_{m=l+1}^{P-1}\exp\left(\xi\mu_p+\xi\mu_m+\xi^2\frac{\sigma_p^2}{2}+\xi^2\frac{\sigma_m^2}{2}\right)\end{aligned}. \quad (36)$$

The relation of mean and variance of the log normal variable to that of corresponding normal variable can be given as

$$\mu_\beta=\exp\left(\mu_z+\frac{\sigma_z^2}{2}\right),\quad\sigma_\beta^2=\exp\left(2\mu_z+2\sigma_z^2\right). \quad (37)$$

Hence, the mean and variance, μ_z and σ^2_z are given by

$$\mu_z=\ln\left(\mu_\beta^2/\sigma_\beta\right);\quad\sigma_z^2=\ln\left(\sigma_\beta^2/\mu_\beta^2\right). \quad (38)$$

Effectively, the whole OFDM sample would be attenuated by a factor of β^2, which is log normally distributed [24].

$$\text{Now,}\quad E[\beta^2]=\mu_{final}=\exp\left(2\mu_z+2\sigma_z^2\right). \quad (39)$$

Since the channel in consideration is time invariant, thus the absolute value of the SNR would be scaled down by a factor of μ_{final} [27, pp. 816-820]. Thus, the relation between the SNR in UWB channel $SNR(uwb)$ and the SNR in AWGN channel $SNR(awgn)$ can be expressed as

$$SNR(uwb)=\mu_{final,CM}*SNR(awgn) \quad (40)$$

where $\mu_{final,CM} = \sum_{r=1}^{r_{\max}} \mu_{final,r}$, $r_{\max}$ is no. of channel realizations.

In a fading channel, since 100% of the transmitted power can never be captured at the receiver, $SNR(uwb)$ will inevitably be lesser than $SNR(awgn)$. Hence, the value of μ_{final} is expected to be less than 1. This fact is validated by the simulation results in the Section 5.2.3 (Comparing Fig. 8 and Fig. 9 with Fig. 7). Recalling (23), CRLB for variance of estimation error in a UWB channel may be defined as

$$Var\left(\hat{\varepsilon}_{b_{in}}(L)\right)(uwb) = N^2 / \{ SNR(uwb) M (L-1) (2\pi d N_s)^2 \}. \quad (41)$$

It is evident from (41) that the CRLB in UWB environment can be modeled as a shifted version of the CRLB in AWGN channel caused by a reduction in the SNR (dB) by a factor, which is constant for a particular CM. The four different CMs, CM1-CM4 are expected to exhibit different values of μ_{final} and hence separate CRLBs are derived for each case. Since $SNR(uwb) < SNR(awgn)$, CRLB of all four CMs are expected to be higher than the CRLB in AWGN channel. Also CM1 (LOS channel over a distance of 0-4m) is expected to give the best performance concerned to CRLB because of the relatively low energy dissipation. The other channels being non-LOS would lead to higher levels of energy dissipation and are expected to exhibit significantly worse performance. Simulation results in Section 5 also verify the same.

5. Simulation Results and Discussions

5.1 Simulation Environment

Simulations are carried out to study the performance of the FO estimation algorithm for MB-OFDM systems using TFI pattern 1 [17] in UWB CMs CM1-CM4 and AWGN in BG 1. Relevant parameters from ECMA-368 standard for MB-OFDM are considered for the simulation study. We have considered 1000 noisy realizations in each of the 100 UWB channels. We estimated the channel using the least square (LS) estimate during CE sequence (25th-30th OFDM symbol of the frame format) of the preamble. We have considered different CIRs and the NCFOs of 0.033, 0.038, and 0.043 in band1, band2, and band3, respectively. Performance analysis of MB-OFDM system is carried out with TCFS in all UWB CMs.

5.2 BER Performance

The coarse FO is estimated using TCFS for AWGN and UWB channels using several consecutive OFDM symbols (L = 2, 3 4, 5, and 6) in the preamble for MB-OFDM system. Fig. 3 to Fig. 6 present the BER vs. Eb/No plots for TCFS with L = 2, 3, and 6 in UWB CM1-CM4 respectively. From Fig. 3 to Fig. 6, the following observations can be made:

At the BER of 10^{-3},

- $L = 6$ gives 7.6 dB, 8.4 dB, 8.6 dB, and 8.5 dB improvements in Eb/No compared to the cases of $L = 2$ in CM1-CM4 respectively.
- Compared to $L = 3$, $L = 6$ improves Eb/No by 3.4 dB, 4.2 dB, 4.4 dB, and 4.2 dB in CM1-CM4 respectively.

At the BER of 2×10^{-4},

- With $L = 6$, Eb/No improves by 8.1 dB, 8.2 dB, 8.4 dB, and 8.2 dB in CM1-CM4 respectively compared to $L = 2$.
- $L = 6$ shows Eb/No improvement of 4.4 dB in both CM1 and CM3, 4.3 dB in CM2 and 4.2 dB in CM4 compared to the case of $L = 3$.

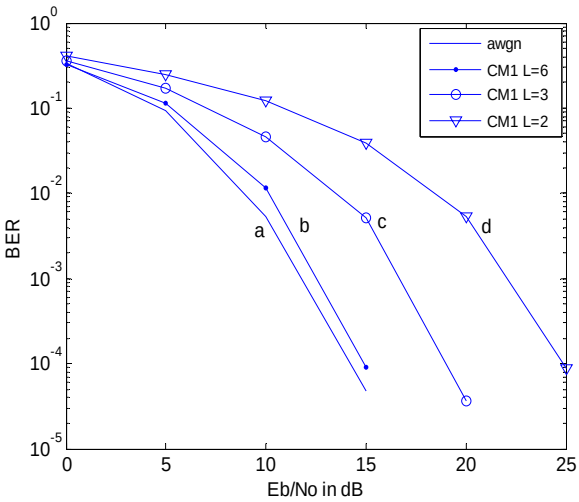

Fig. 3. BER vs. Eb/No for: a) AWGN with L=6; b) CM1 with L=6; c) CM1 with L=3 and d) CM1 with L=2.

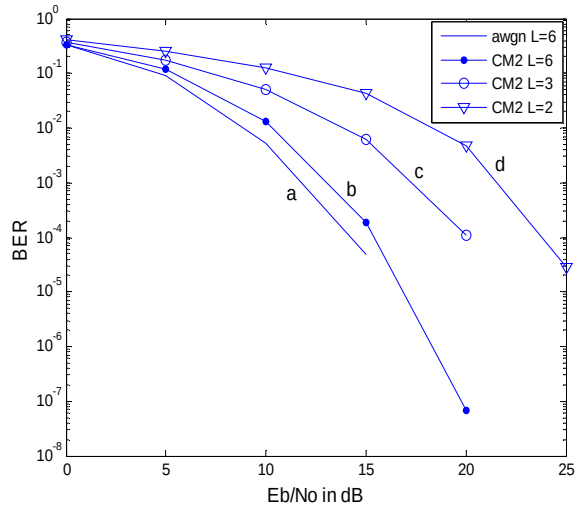

Fig. 4. BER vs. Eb/No for: a) AWGN with L=6; b) CM2 with L=6; c) CM2 with L=3 and d) CM2 with L=2.

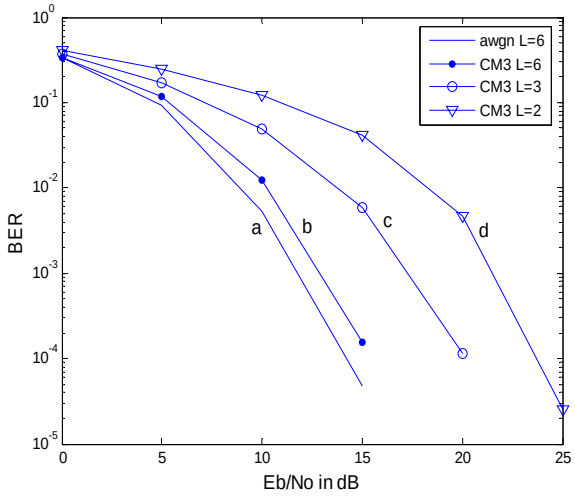

Fig. 5. BER vs. Eb/No for: a) AWGN with L=6; b) CM3 with L=6; c) CM3 with L=3 and d) CM3 with L=2.

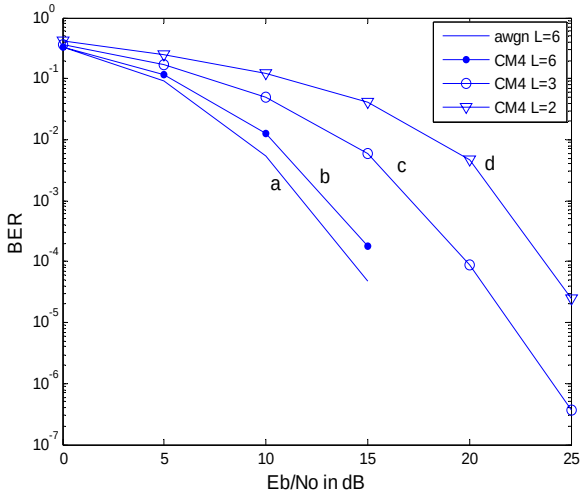

Fig. 6. BER vs. Eb/No for: a) AWGN with L=6; b) CM4 with L=6; c) CM4 with L=3 and d) CM4 with L=2.

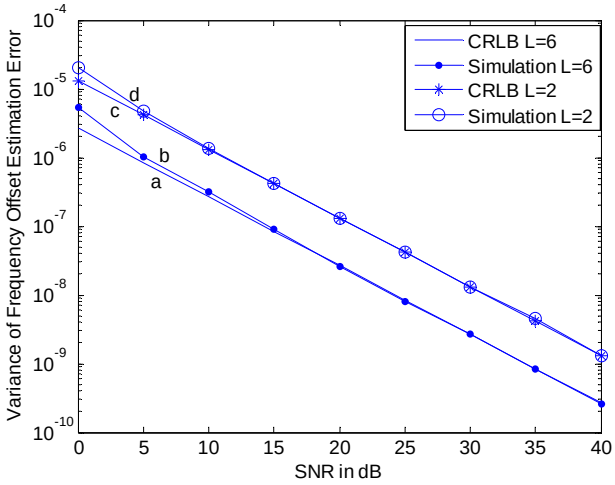

Fig. 7. Variance of frequency offset estimation error vs. SNR: a) CRLB calculated with L=6; b) simulation with L=6; c) CRLB calculated with L=2; d) simulation with L=2 for MB-OFDM system in AWGN channel.

5.3 CRLB in AWGN Channel

Here we compare the calculated CRLB with the variance of error obtained by simulation with TCFS for an AWGN channel. Fig. 7 shows the change of variance of the FO estimation error of TCFS vs. SNR for various values of L, viz. 2, and 6. It also includes the error variance of FO estimate and the CRLB of the error variance for TCFS for L = 2 and 6.

From Fig. 7 the following observations can be made:

- As expected, the variance of FO estimation error decreases with increase in L. However, a lower value of L is desirable in practice to reduce the system computational complexity.
- It is observed that the error variance as per our scheme is very close to the corresponding CRLB calculated.

5.4 CRLB in UWB Channel

It is discussed in Section 4.2 that, the effective SNR in UWB channel is the scaled down version of the absolute SNR in AWGN channel by a constant of μ_{final}.

Simulation is carried out to estimate the exact value of $\mu_{final,CM}$ for CMs. The value of μ_p was obtained for each p across all the 100 realizations of the four CMs using (25) and (30). The values of the cluster arrival time T_j and the ray arrival time $\tau_{i,j}$ were obtained from [18]. The value of Ω_0, defined as the "mean energy of the first path of the first cluster" in [18], is obtained by considering the first sample of the IR in each realization of CM1. However, for the non-LOS CMs, cluster power fails to show a sharp onset. It is rather observed that the power increases gradually till a local maximum is reached. Thus, merely taking the mean energy of the first path of the first cluster would lead to inaccurate results. So, the Geometric Mean of all impulse powers leading up to local maximum is considered to calculate the value of Ω_0 here.

Thereafter, the means and variances namely μ_β, σ^2_β, μ_z and σ^2_z are obtained from (35), (36) and (39), (40). The value of μ_{final} is thereby calculated individually for each of the realizations of a CM. The final mean value for each CM $\mu_{final,CM}$ is then calculated by averaging μ_{final} of 100 realizations.

Fig. 8 shows the error variance of FO estimate obtained from the simulation and the CRLB of the error variance with TCFS for L=2 in UWB CMs, CM1 and CM3. We compare the simulation results with CRLB for CM2 and CM4 for L=2 in Fig. 9. Observation can be made from Fig. 8 and Fig. 9 is:

- The figures depict that error variances with TCFS closely match to their corresponding CRLBs in all UWB CMs.

A similar kind of decrement in error variance is also noticed for L = 3, 4 and 6; but not reported here to reduce the redundancy.

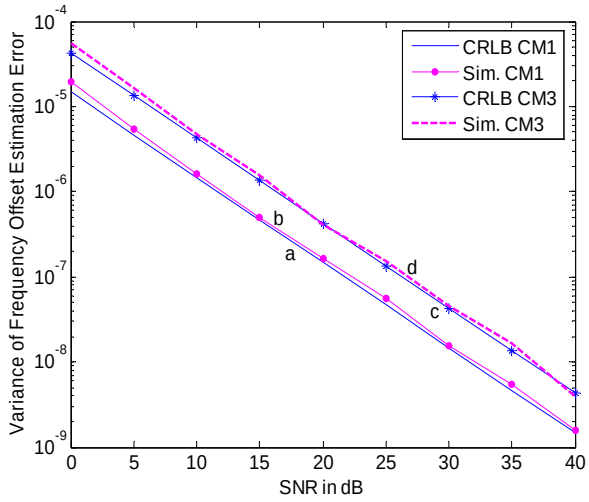

Fig. 8. Variance of frequency offset estimation error vs. SNR with L=2: a) CRLB calculated in CM1; b) simulation in CM1; c) CRLB calculated in CM3; d) simulation in CM3 with TCFS.

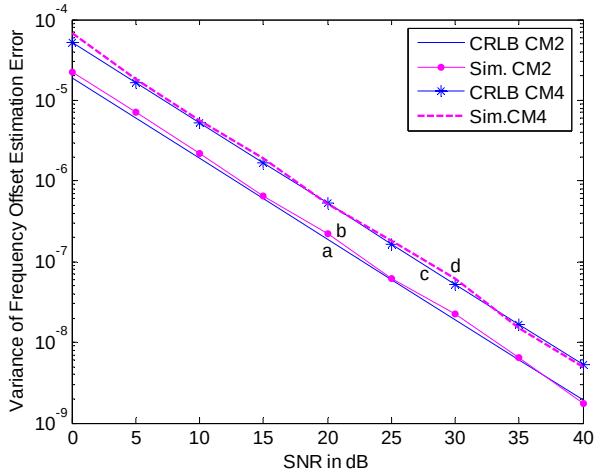

Fig. 9. Variance of frequency offset estimation error vs. SNR with L=2: a) CRLB calculated in CM2; b) simulation in CM2; c) CRLB calculated in CM4; d) simulation in CM4 with TCFS.

We have compared the performance of error variance of TCFS with reported results of Yak et al. [10] for CM1 and CM2. Comparisons in CM3 and CM4 are not provided here as the performances of the estimator [10] in these channels are not reported in [10]. Fig. 10 and Fig. 11 present the comparative study of TCFS with [10] for CM1 and CM2 respectively for L = 2. Our main observations from these comparative studies (Fig. 10 and Fig. 11) are as follows:

- For CM1 both CRLB and simulated error variance are lower than [10] for all SNRs of interest.
- For CM1 SNR improves by 5.8 dB at both the error variances of 10^{-6} and 10^{-7} in the low SNR zone (≤ 8 dB).
- In CM2, for SNR > 15 dB, the simulated error variances and CRLB for both TCFS and [10] match closely.
- CM2 shows SNR improvement of 4.8 dB and 4.0 dB at the error variances of 10^{-6} and 10^{-7} respectively in the low SNR zone (≤8 dB).

Hence, it is noticed that in both the channels, for SNR ≤ 8 dB, TCFS performs better than [10].

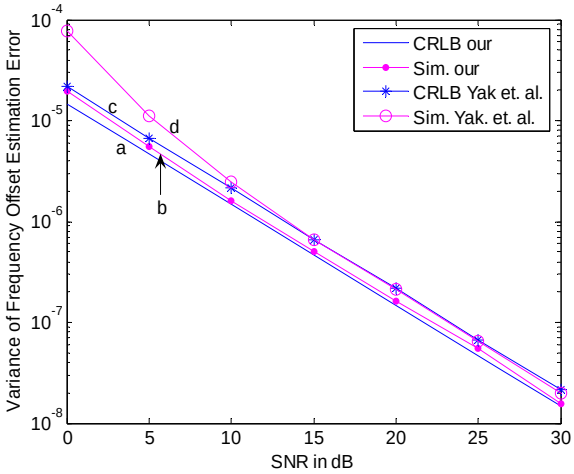

Fig. 10. Variance of frequency offset estimation error vs. SNR with L=2 in CM1: a) CRLB calculated by TCFS; b) simulation by TCFS; c) CRLB calculated by Yak et al. [10]; d) simulation by Yak et al. [10].

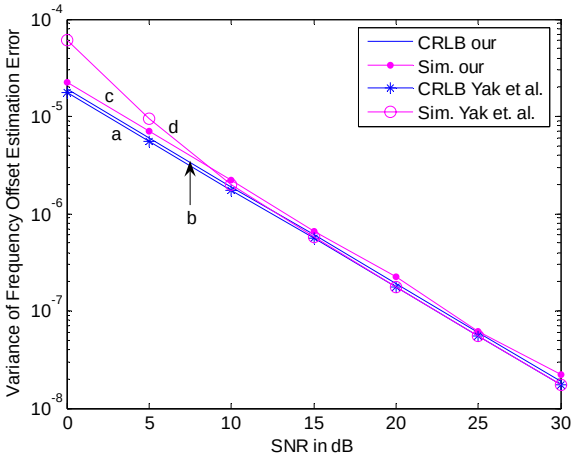

Fig. 11. Variance of frequency offset estimation error vs. SNR with L=2 in CM2: a) CRLB calculated by Yak et al. [10]; b) CRLB calculated by TCFS; c) simulation by TCFS; d) simulation by Yak et al. [10].

6. Conclusions

We present an efficient near-optimum system performance (AWGN performance) achieving, satisfactory low-complexity synchronizer TCFS for MB-OFDM UWB systems and show the BER performances under different UWB realistic channel environments CM1-CM4. We also derive CRLB for TCFS and compare the simulated error

variance to that of the theoretical calculations. TCFS shows excellent attribute in terms of reduction of error variance compared to the existing results in literature [10] as well as achieving near-optimum BER performances with higher no. of OFDM symbols (L values). With large no. of OFDM symbols say L= 6, TCFS achieves an Eb/No improvements of around 8 dB in all CMs compared to minimum value of L i.e. 2 at the BER of 2×10^{-4} with a reasonable complexity.

The novelty of TCFS lies in improving the system performance by reducing the estimation error variance through several iterations performed over a number of OFDM symbols utilized for estimation per band. Furthermore, the proposed estimator performs better than the ML estimator reported in [10] in the low SNR zone (≤ 8 dB) in both CM1 and CM2. This is an attractive feature for UWB based system as they are expected to perform in low SNR zone in practice. Thus TCFS has good potential for application in practical UWB receiver for WPAN. Moreover, to the best of our knowledge, CRLB for UWB CM3 and CM4 are reported for the first time in literature in this paper.

This work can further be extended for time varying channels considering the presence of occasional fast moving scatterers in channel which can cause abrupt channel change blocking some of existing ones. It can also be analyzed considering jointly the timing error; frequency offset error, and the presence of jitter in above described scenario.

Appendix A

Calculation of Variance of Frequency Offset Estimation

Following (4) we can write for initial band of estimation *'b_{in}'*

$$e^{j2\pi\varepsilon_{b_{in}}(n+N_g+lN_s)/N}\, x_{b_{in}}(l,n)=x'_{b_{in}}(l,n)\,. \tag{42}$$

Hence, the n-th sample of (l+1)-th OFDM symbol $x_{b_{in}}(l+1,n)$ can be related with $x'_{b_{in}}(l,n)$ as

$$x'_{b_{in}}(l+1,n)=x_{b_{in}}(l,n)\,e^{j2\pi\varepsilon_{b_{in}}dN_s/N}\,. \tag{43}$$

Therefore (4) can be rewritten as

$$y_{b_{in}}(l,n)=x'_{b_{in}}(l,n)+w_{b_{in}}(l,n)\,. \tag{44}$$

Similarly

$$y_{b_{in}}(l+1,n)=x'_{b_{in}}(l,n)e^{j2\pi\varepsilon_{b_{in}}dN_s/N}+w_{b_{in}}(l+1,n)\,. \tag{45}$$

The FO $\hat{\varepsilon}_{b_{in}}(l)$ estimated from l-th and (l+1)-th OFDM symbol in band *'b_{in}'*, is expressed as

$$\hat{\varepsilon}_{b_{in}}(l)=\frac{1}{(2\pi dN_s/N)}\tan^{-1}\left[\frac{\sum_{n=0}^{M-1}\mathrm{Im}\left\{y^*_{b_{in}}(l,n)\,y_{b_{in}}(l+1,n)\right\}}{\sum_{n=0}^{M-1}\mathrm{Re}\left\{y^*_{b_{in}}(l,n)\,y_{b_{in}}(l+1,n)\right\}}\right]$$

$$=\left\{1/(2\pi dN_s/N)\right\}$$

$$\tan^{-1}\left\{\frac{\mathrm{Im}[(x^*_{b_{in}}(l,n)+w^*_{b_{in}}(l,n))(x'_{b_{in}}(l,n)e^{j2\pi\varepsilon_{b_{in}}dN_s/N}+w_{b_{in}}(l+1,n))]}{\mathrm{Re}[(x'^*_{b_{in}}(l,n)+w^*_{b_{in}}(l,n))(x'_{b_{in}}(l,n)e^{j2\pi\varepsilon_{b_{in}}dN_s/N}+w_{b_{in}}(l+1,n))]}\right\} \tag{46}$$

Now, for the estimation error $\left|\hat{\varepsilon}_{b_{in}}(l,n)-\varepsilon_{b_{in}}\right|\ll N/2\pi dN_s$, and high SNR, estimation error is approximated as [10]

$$\hat{\varepsilon}_{b_{in}}(l)-\varepsilon_{b_{in}}\approx\left\{1/(2\pi dN_s/N)\right\}$$

$$\left\{\frac{\sum_{n=0}^{M-1}\mathrm{Im}[w^*_{b_{in}}(l,n)x'_{b_{in}}(l,n)+x'^*_{b_{in}}(l,n)e^{-j2\pi\varepsilon_{b_{in}}dN_s/N}w_{b_{in}}(l+1,n)]}{\sum_{n=0}^{M-1}\left|x'_{b_{in}}(l,n)\right|^2}\right\}. \tag{47}$$

For estimation using L OFDM symbols

$$\hat{\varepsilon}_{b_{in}}(L)-\varepsilon_{b_{in}}\approx\left\{1/(2\pi dN_s/N)\right\}$$

$$\left\{\frac{\sum_{l=1}^{L-1}\sum_{n=0}^{M-1}\mathrm{Im}[w^*_{b_{in}}(l,n)x'_{b_{in}}(l,n)+x'^*_{b_{in}}(l,n)e^{-j2\pi\varepsilon_{b_{in}}dN_s/N}w_{b_{in}}(l+1,n)]}{\sum_{l=1}^{L-1}\sum_{n=0}^{M-1}\left|x'_{b_{in}}(l,n)\right|^2}\right\}. \tag{48}$$

The mean of the above expression is found to be zero given $\varepsilon_{b_{in}}$ and $\{y_{b_{in}}(n)\}$. The variance of estimation for two consecutively received OFDM symbols is thus given by

$$\mathrm{var}(\hat{\varepsilon}_{b_{in}}(l))=N^2/\left\{(2\pi dN_s)^2\,M(SNR)\right\} \tag{49}$$

where $SNR = E_S/\sigma^2$ and E_S is the transmitted signal power over one subcarrier of an OFDM symbol.

For estimation over L OFDM symbols, the variance of estimation can be obtained as

$$\mathrm{var}(\hat{\varepsilon}_{b_{in}}(L))=N^2/\left\{(2\pi dN_s)^2(L-1)M(SNR)\right\}. \tag{50}$$

Appendix B

Computational Complexity Analysis for TCFS

Here, we compute the computational complexity of TCFS algorithm for one band. We define: T_{total} is the total time of 'busy period' during which the estimation runs, T_{OFDM} is the time period of one OFDM symbol (=312.5 nsec.). It is to be noted that T_{total} gives the time period over which we get L OFDM symbols and it depends

on the periodicity of same band repetition i.e. on the TFI pattern opted for transmission.

Tab. 1 tabulates the calculated T_{total} for different TFI patterns for both L = odd and L = even.

In the FO estimation algorithm we need to perform basically three main operations: complex conjugate multiplication, extraction of phase, and averaging. Assuming, conjugation is trivial, within the total time period of T_{total}, we need to do $(L\text{-}1)N$ nos. of complex multiplications.

We will be using CORDIC block for extraction of phase. Let, W is the no. of stages of the CORDIC block. Hence, the no. of addition for each sample is $\approx 2W$. Therefore, total no. of addition required for the purpose of phase extraction is

$$2W(L-1). \tag{51}$$

In the averaging process, we assume that the division is trivial. Numbers of samples over which the averaging will run are $(L\text{-}1)N$. So, the no. of addition required for averaging is

$$(L-1)N-1 \tag{52}$$

Now, total multiplication complexity for TCFS is

$$(L-1)N/T_{\text{total}} \text{ multiplications/sec} \tag{53}$$

and, total additional complexity for TCFS is

$$\begin{aligned}&\{(L-1)2W+(L-1)N-1\}/T_{\text{total}}\\ &=\{(2W+N)(L-1)-1\}/T_{\text{total}} \text{ additions/sec}\end{aligned} \tag{54}$$

TFI no.	T_{total}		Value of d
	L= even	L= odd	
1	$((L-1)d+1)T_{\text{OFDM}}$	$((L-1)d+1)T_{\text{OFDM}}$	3
2	-do-	-do-	3
3	$\left\{\left\lfloor\frac{L-1}{2}\right\rfloor 6+2\right\}T_{\text{OFDM}}$	$\left\{\left\lfloor\frac{L-1}{2}\right\rfloor 6+1\right\}T_{\text{OFDM}}$	1 & 5
4	-do-	-do-	1 & 5
5	LT_{OFDM}	LT_{OFDM}	1
6	-do-	-do-	1
7	-do-	-do-	1
8	$((L-1)d+1)T_{\text{OFDM}}$	$((L-1)d+1)T_{\text{OFDM}}$	2
9	-do-	-do-	2
10	-do-	-do-	2

Tab. 1. Expressions of T_{total} for different TFI pattern for L= odd and L= even.

Appendix C

Calculation Details of the Cramer Rao Lower Bound (CRLB)

Taking the second order partial derivatives of $f(Z_{b_{in}}(l,n),\alpha)$ (20) yield

$$\begin{aligned}\frac{\partial^2 \ln\left(f\left(Z_{b_{in}}(l,n);\alpha\right)\right)}{\partial \varepsilon_{b_{in}}^2} &= -\frac{1}{\sigma^2}\left(2\pi d\frac{N_s}{N}\right)^2 \sum_{n=0}^{M-1}\left\{A^2\cos^2\left(2\pi\varepsilon_{b_{in}} d\frac{N_s}{N}\right)\right.\\ &\left.+\bar{w}_{in}A\cos\left(2\pi\varepsilon_{b_{in}} d\frac{N_s}{N}\right)+A^2\sin^2\left(2\pi\varepsilon_{b_{in}} d\frac{N_s}{N}\right)+\bar{w}_{qp}A\sin\left(2\pi\varepsilon_{b_{in}} d\frac{N_s}{N}\right)\right\}\end{aligned} \tag{55}$$

Expected value of second order partial derivative is

$$\begin{aligned}&E\left\{\frac{\partial^2 \ln\left(f\left(Z_{b_{in}}(l,n);\alpha\right)\right)}{\partial^2 \varepsilon_{b_{in}}^2}\right\} = \\ &-\frac{1}{\sigma^2}\left(2\pi d\frac{N_s}{N}\right)^2 \sum_{n=0}^{M-1} A^2 = -\frac{1}{\sigma^2}\left(2\pi d\frac{N_s}{N}\right)^2 MA^2\end{aligned} \tag{56}$$

The second order partial derivatives of $f(Z_{b_{in}}(l,n),\alpha)$ with respect to A yield

$$\begin{aligned}&\frac{\partial^2 \ln\left(f\left(Z_{b_{in}}(l,n);\alpha\right)\right)}{\partial A^2} = \\ &-\frac{1}{\sigma^2}\left(\sum_{n=0}^{M-1}\cos^2\left(2\pi\varepsilon_{b_{in}} d\frac{N_s}{N}\right)+\sin^2\left(2\pi\varepsilon_{b_{in}} d\frac{N_s}{N}\right)\right)\end{aligned} \tag{57}$$

Expected value of second order partial derivative is

$$E\left\{\frac{\partial^2 \ln\left(f\left(Z_{b_{in}}(l,n);\alpha\right)\right)}{\partial A^2}\right\} = -\frac{M}{\sigma^2}. \tag{58}$$

Now

$$\begin{aligned}&\frac{\partial^2 \ln\left(f\left(Z_{b_{in}}(l,n);\alpha\right)\right)}{\partial A\partial \varepsilon_{b_{in}}}\\ &= -\frac{1}{\sigma^2}\left(2\pi d\frac{N_s}{N}\right)\sum_{n=0}^{M-1}\left\{A\sin\left(2\pi\varepsilon_{b_{in}} d\frac{N_s}{N}\right)\right.\\ &\cos\left(2\pi\varepsilon_{b_{in}} d\frac{N_s}{N}\right)+\bar{w}_{in}\sin\left(2\pi\varepsilon_{b_{in}} d\frac{N_s}{N}\right)+\\ &\left.A\cos\left(2\pi\varepsilon_{b_{in}} d\frac{N_s}{N}\right)\sin\left(2\pi\varepsilon_{b_{in}} d\frac{N_s}{N}\right)+\bar{w}_{qp}\left(2\pi\varepsilon_{b_{in}} d\frac{N_s}{N}\right)\right\}\end{aligned} \tag{59}$$

which results in

$$E\left\{\frac{\partial^2 \ln\left(f\left(Z_{b_{in}}(l,n);\alpha\right)\right)}{\partial A \partial \varepsilon_{b_{in}}}\right\} = 0 \cdot \tag{60}$$

Again

$$\begin{aligned}&\frac{\partial^2 \ln\left(f\left(Z_{b_{in}}(l,n);\alpha\right)\right)}{\partial \varepsilon_{b_{in}} \partial A}\\ &= -\frac{1}{\sigma^2}\left(2\pi d\frac{N_S}{N}\right)\sum_{n=0}^{M-1}\left\{A\sin\left(2\pi\varepsilon_{b_{in}} d\frac{N_S}{N}\right)\cos\left(2\pi\varepsilon_{b_{in}} d\frac{N_S}{N}\right)\right.\\ &+\bar{w}_{in}\sin\left(2\pi\varepsilon_{b_{in}} d\frac{N_S}{N}\right) - A\cos\left(2\pi\varepsilon_{b_{in}} d\frac{N_S}{N}\right)\\ &\left.\sin\left(2\pi\varepsilon_{b_{in}} d\frac{N_S}{N}\right) - \bar{w}_{qp}\cos\left(2\pi\varepsilon_{b_{in}} d\frac{N_S}{N}\right)\right\}\end{aligned} \tag{61}$$

that yields

$$E\left\{\frac{\partial^2 \ln\left(f\left(Z_{b_{in}}(l,n);\alpha\right)\right)}{\partial \varepsilon_{b_{in}} \partial A}\right\} = 0 \cdot \tag{62}$$

Unbiased CRLB for the variance of unknown parameter estimates are obtained from diagonal elements of Inverse FIM $J(\alpha)$ [23] given as

$$\begin{aligned}&J(\alpha)\\ &= \begin{bmatrix} -E\left[\frac{\partial^2 \ln\left(f\left(Z_{b_{in}}(l,n);\alpha\right)\right)}{\partial A^2}\right] & -E\left[\frac{\partial^2 \ln\left(f\left(Z_{b_{in}}(l,n);\alpha\right)\right)}{\partial A \partial \varepsilon_{b_{in}}}\right] \\ -E\left[\frac{\partial^2 \ln\left(f\left(Z_{b_{in}}(l,n);\alpha\right)\right)}{\partial \varepsilon_{b_{in}} \partial A}\right] & -E\left[\frac{\partial^2 \ln\left(f\left(Z_{b_{in}}(l,n);\alpha\right)\right)}{\partial \varepsilon_{b_{in}}^2}\right] \end{bmatrix}\\ &= \begin{bmatrix} -M^2/\sigma^2 & 0 \\ 0 & -\frac{1}{\sigma^2}\left(2\pi d N_S/N\right)^2 MA^2 \end{bmatrix}\end{aligned} \tag{63}$$

CRLB for variance of FO estimation is given as

$$Var\left(\hat{\varepsilon}_{b_{in}}(l)\right) = \frac{M\sigma^2}{A^2 M^2\left[2\pi d\frac{N_s}{N}\right]^2} \tag{64}$$

Substituting signal-to-noise-ratio $SNR = A^2/\sigma^2$ and on simplification we get

$$Var\left(\hat{\varepsilon}_{b_{in}}(l)\right) = N^2/\{(SNR)M\left(2\pi d N_s\right)^2\}. \tag{65}$$

References

[1] BATRA, A., BALAKRISHNAN, J., AIELLO, G. R., FOERSTER, J. R., DABAK, A. Design of Multi-band system for realistic UWB channel environment. *IEEE Transactions on Microwave Theory and Techniques*, Sept. 2004, vol. 52, no. 9, p. 2123 - 2138.

[2] MOOSE, P. H. A technique for orthogonal frequency division multiplexing frequency offset correction. *IEEE Transactions on Communications,* Oct. 1994, vol. 42, no. 10, p. 2908 - 2914.

[3] CLASSEN, F., MEYR, H. Frequency synchronization algorithms for OFDM systems suitable for communication over frequency selective fading channels. In *Proceedings of the IEEE Veh. Technol. Conf.* Stockholm (Sweden), Jun. 1994, p. 1655 to 1659.

[4] SCHMIDL, T. M., COX, D. C. Robust frequency and timing synchronization for OFDM. *IEEE Transactions on Communications*, Dec. 1997, vol. 45, p. 1613 - 1621.

[5] HSIEH, M. H., WEI, C. H. A low-complexity frame synchronization and frequency offset compensation scheme for OFDM systems over fading channels. *IEEE Transactions on Vehicular Technology*, Sep. 1999, vol. 48, no. 5.

[6] MORELLI, M., MENGALI, U. An improved frequency offset estimator for OFDM applications. *IEEE Communication Letters*, March 1999, vol. 3, no. 3.

[7] TSAI, P. Y., KANG, H. Y., CHIUEH, T. D. Joint weighted least-squares estimation of carrier-frequency offset and timing offset for OFDM systems over multipath fading channels. *IEEE Transactions on Vehicular Technology*, Jan. 2005, vol. 54, no. 1, p. 211 - 223.

[8] ZHU, J., LEE, W. Carrier frequency offset estimation for OFDM systems with null subcarriers. *IEEE Transactions on Vehicular Technology*, Sept. 2006, vol. 55, no. 5, p. 1677 - 1690.

[9] KATO, Y., HIRATSUKA, Y., SANADA, Y. Frequency offset compensation scheme for MB-OFDM by frequency spreading. In *Proceedings of the IEEE ISPACS.* Hong Kong, Dec. 13-16, 2005, p. 209 - 212.

[10] YAK, C. W., LEI, Z., TJHUNG, T. T. Maximum likelihood frequency offset estimation and Cramer Rao bound for ultra-wideband (UWB) multi-band OFDM (MB-OFDM) systems. In *Proceedings of the IEEE VTC 2006-spring.* Melbourne (Australia), 2006, vol. 5, p. 2373 - 2377.

[11] LI, Y., JACOBS, T., MINN, H. Frequency offset estimation for MB-OFDM-based UWB systems. In *Proceedings of the IEEE ICC.* Istanbul (Turkey), June 2006, vol. 10, p. 4729 - 4734.

[12] JACOBS, T., LI, Y., MINN, H., RAJATHEVA, R. M. A. P. Synchronization in MB-OFDM-based UWB systems. In *Proc. of the IEEE ICC.* Glasgow (Scotland), June 24-28, 2007, p. 1071 - 1076.

[13] LI, Y., MINN, H., WIN, M. Z. Frequency offset estimation for MB-OFDM –based UWB systems in time-variant channels. In *Proceedings of the IEEE WCNC.* Hong Kong, March 11-15, 2007, p. 1020 – 1025.

[14] PNG, K. B., PENG, X., CHATTONG, S., FRANCIS, H. T., CHIN, F. Joint carrier and sampling frequency offset estimation for MB-OFDM UWB system. In *Proceedings of the IEEE RWS.* Orlando (FL), Jan 22-24, 2008, p. 29 - 32.

[15] SEN, D., CHAKRABARTI, S., RAJA KUMAR, R. V. An efficient frequency offset estimation scheme for Multi-Band OFDM Ultra-Wideband systems. In *Proceedings of the IEEE VTC 2008-spring.* Singapore, May 11-14, 2008, p. 973 - 977.

[16] SEN, D., CHAKRABARTI, S., RAJA KUMAR, R. V. A new frequency offset estimation scheme for Ultra-Wideband MB-OFDM systems. In *Proceedings of the IEEE ICACT.* Phoenix Park (Korea), Feb. 17-20, 2008, vol. 3, p. 1929 - 1934.

[17] ECMA-368, High Rate Ultra Wideband PHY and MAC standard, 2nd edition. Dec. 2007. Available at: <http://www.ecma-international.org/publications/standards/Ecma-368.htm>

[18] FOERSTER, J. Channel modeling sub-committee report final. Document IEEE P802.15-02/490r1-SG3a, Feb. 2003.

[19] QUI, R. C. A study of the Ultra-Wideband Wireless Propagation Channel and Optimum UWB Receiver Design. *IEEE Journal on Selected Areas in Communications*, Dec. 2002, vol. 20, no. 9, p. 1628 - 1637.

[20] GENG, S., VAINIKAINEN, P. Frequency and bandwidth dependency of UWB propagation channels. In *Proceedings of the IEEE PIMRC.* Helsinki (Finland), Sept. 11-14, 2006.

[21] MOLISCH, A. F. Ultrawideband propagation channels-theory, measurement, and modelling. *IEEE Transaction on Vehicular Technology*, Sept. 2005, vol. 54, no. 5, p.1528 - 1545.

[22] SEN, D., CHAKRABARTI, S., RAJA KUMAR, R. V. Mathematical analysis of signal propagation in ultra-wideband transceiver system with frequency offset correction. In *Proceedings of the IEEE PIMRC.* Cannes (France), Sept. 15-18, 2008. (In press).

[23] KAY, S. M. *Fundamentals of Statistical Signal Processing: Estimation Theory*. Prentice Hall PTR, 1993.

[24] LIU, H. Error performance of a pulse amplitude and position modulated Ultra-Wideband system over lognormal fading channels. *IEEE Communication Letters*, Nov. 2003, vol. 7, no. 11, p. 531 - 533.

[25] BEAULIEU, N. C., ABU-DAYYA, A. A., MCLANE, P. J. Estimating the distribution of a sum of independent lognormal random variable. *IEEE Trans. Communications*, Dec. 1995, vol. 43, p. 2869 - 2873.

[26] CARDIERI, P., RAPPAPORT, T. S. Statistics of the sum of lognormal variables in Wireless Communications. In *Proceedings of the IEEE VTC 2000-spring.* Tokyo (Japan), May 15-18, 2000, vol. 3, p. 1823 - 1827.

[27] PROAKIS, J. G. *Digital Communications.* 4th ed. McGraw Hill International Edition, 2001.

About Authors...

Debarati SEN, a National Doctoral Fellow, India is currently associated with the G. S. S. School of Telecommunications, Indian Institute of Technology Kharagpur, India as a Research Scholar working towards her Ph.D degree. Her present interest includes Wireless Communication Systems, mostly, Ultra-Wideband (UWB) Communications, MB-OFDM, Synchronization etc. She has published a few related papers in IEEE. A university topper in her masters in engineering, Debarati possesses experience at different levels in different institutions/industries. She was a Lecturer in an Engineering College prior to join IIT-Kharagpur. She is also a student member of IEEE and an associate member of IE(I).

Rahul DASGUPTA has graduated in Electronics and Electrical Communication Engg. from Indian Institute of Technology Kharagpur, India in 2008. Currently, he is pursuing PGDM at Indian Institute of Management, Calcutta, India. He has worked in the field of Carrier Frequency Synchronization in OFDM systems modeled for Ultra-Wideband (UWB) Communication and its Applications as a part of B.Tech dissertation.

Saswat CHAKRABARTI has been with the G. S. S. School of Telecommunications, Indian Institute of Technology Kharagpur, India, since 1991, where he is a Professor and present Head. He received M.Tech. and Ph.D both in Electronics & Electrical Communications Engg. from IIT Kharagpur in 1985 and 1992 respectively. His research focuses on Wireless Communications, Error Control Coding, Digital Modulation schemes, Mobile Ad-hoc Networks and Bio-telemetry. Dr. Chakrabarti received Design Contest Award for Best Design Entry in 18th Int. Conf. on VLSI Design and 4th Int. Conf. on Embedded Systems, 2005. He published more than 60 papers in international journals and conference proceedings. He has also been handling more than 20 consultancy and sponsored research and technology development projects. He is a member of IEEE.

R. V. RAJA KUMAR is now a Professor, Department of Electronics and Electrical Communication Engineering, Indian Institute of Technology Kharagpur, India. He received M.Tech. in Microwave & Radar Engineering and Ph.D. in Digital Signal Processing in 1982 and 1987 respectively from IIT-Kharagpur. His research interests include Digital Signal Processing, Wireless Communications, Detection and Estimation theory and VLSI for Communication Systems. He published about 100 technical papers in international journals and conference proceedings. Dr. Raja Kumar was awarded the BOYS-CAST research grant from the Department of Science and Technology, Government of India in 1987. He received the first prize in the 1984 IEEE Region 10 Graduate Paper Contest. He served as a member of several committees of the central government bodies, was instrumental in the initiation and a founding member of the Indest Consortium. He has also been handling a number of consultancies and sponsored research and technology development projects. He is a senior member of IEEE.